



NIH Public Access

Author Manuscript

Proteins. Author manuscript; available in PMC 2014 March 01.

Published in final edited form as:
Proteins. 2013 March ; 81(3): 365–376. doi:10.1002/prot.24192.

Prediction, Refinement and Persistency of Transmembrane Helix Dimers in Lipid Bilayers using Implicit and Explicit Solvent/Lipid Representations: Microsecond Molecular Dynamics Simulations of ErbB1/B2 and EphA1

Liqun Zhang¹, Alexander J. Sodt², Richard M. Venable², Richard W. Pastor², and Matthias Buck^{1,3,4,5,*}

¹Department of Physiology and Biophysics, Case Western Reserve University, Cleveland, Ohio 44106

²Lab. of Computational Biology, National Heart Lung Blood Institute, National Institutes of Health, Bethesda, MD 20892-9314

³Department of Neuroscience, Case Western Reserve University, Cleveland, Ohio 44106

⁴Department of Pharmacology, Case Western Reserve University, Cleveland, Ohio 44106

⁵Department of Case Comprehensive Cancer Center, Case Western Reserve University, Cleveland, Ohio 44106

Abstract

All-atom simulations are carried out on ErbB1/B2 and EphA1 transmembrane helix dimers in lipid bilayers starting from their solution/DMPC bicelle NMR structures. Over the course of microsecond trajectories, the structures remain in close proximity to the initial configuration and satisfy the great majority of experimental tertiary contact restraints. These results further validate CHARMM protein/lipid force fields and simulation protocols on Anton. Separately, dimer conformations are generated using replica exchange in conjunction with an implicit solvent and lipid representation. The implicit model requires further improvement, and this study investigates whether lengthy all-atom molecular dynamics simulations can alleviate the shortcomings of the initial conditions. The simulations correct many of the deficiencies. For example excessive helix twisting is eliminated over a period of hundreds of nanoseconds. The helix tilt, crossing angles and dimer contacts approximate those of the NMR derived structure, although the detailed contact surface remains off-set for one of two helices in both systems. Hence, even microsecond simulations are not long enough for extensive helix rotations. The alternate structures can be rationalized with reference to interaction motifs and may represent still sought after receptor states that are important in ErbB1/B2 and EphA1 signaling.

Keywords

structure prediction; implicit solvent and lipid; Generalized Born model; replica exchange; receptor tyrosine kinases; solution NMR

*Corresponding author: Matthias Buck, Department of Physiology & Biophysics, Case Western Reserve University, School of Medicine, 10900 Euclid Ave, Cleveland, OH 44106; matthias.buck@case.edu; Phone 216-368-8651.

INTRODUCTION

Transmembrane (TM) proteins play critical roles in cell biology and physiology by transmitting information across cellular barriers. Several mechanisms for such signal transduction have been revealed, ranging from conformational changes in protein channels and pumps to alterations in helix structures that regulate the activity of intra- and extracellular domains in transmembrane receptors¹. Molecular modeling and dynamics simulations are increasingly used to characterize the atomic and energetic details of such mechanisms². TM helix dimers are particularly approachable model systems because they are small, yet contain many key elements of membrane protein structures: tilt with respect to the bilayer, crossing angle and contact surface, as well as competition of lipids and water with protein interactions. For example, studies of the glycophorin A (GPA) helix dimer indicated that protein-protein interactions dominate the structure^{3,4,5} whereas lipid composition (and associated thickness) of the membrane play a more influential roles in other systems^{6,7,8}. Concepts such as hydrophobic (mis-)matching were introduced to describe helix localization and orientation with respect to the membrane. For example, in PG-1 Rui and Im⁹ found that the structures and dynamics of helices can be influenced by the lipid environment. Here, the sequence- and length- specific helix-membrane interactions determined the tilt angle of the TM helix monomer in membranes of different thickness. Conversely, peptides can also affect the lipids that surround them by locally altering bilayer thickness⁴.

TM helices simulated in the presence of explicit lipid and solvent have in some cases been shown to maintain their experimentally derived structures on the tens of nanoseconds time scale (e.g.^{10,11}). However, such all-atom simulations are not yet a suitable method for the prediction of structures from arbitrary initial conditions (e.g., helices on the surface of the bilayer or widely separated helices within the bilayer) because of the limited sampling of conformational space that is possible with currently accessible computers¹². A number of methods have been used to overcome this search problem, with the GPA dimer as a popular example. Mostly these methods utilize simplified representations, often in conjunction with enhanced dynamics protocols. Ponder and colleagues¹³ employed a potential smoothing and search algorithm to predict the packing of the TM helices. In spirit, this approach has evolved into coarse-grained representations, leading recently to accurate predictions by the Sansom group¹² and others¹⁴. An alternative approach has been to use a fully atomistic representation for the protein, while implicit modeling of lipids and solvent is supplemented by forces derived from a database of protein structures^{15,16}. Meanwhile, transmembrane helix assemblies have been successfully designed based upon packing interactions (e.g. ¹⁷). Brownian dynamics, Monte Carlo and molecular docking simulations that treat the GPA helices as essentially rigid units also predict structures that compare well with experiments^{18,19,20,21}. Lazaridis developed an effective energy function for membranes²² and Im and Brooks^{23,24} used the Generalized Born model for an implicit bilayer lipid and solvent representation. However, the experimental GPA structure was only obtained as the major configuration when symmetry restraints were applied to the helices.

While a large number of studies have been carried out on GPA it has also become clear that this system may be a special case, presenting particularly stable helices, strong association, and clear dimerization motifs. We have, therefore, chosen two TM receptor tyrosine kinase dimers as test systems: the ErbB1-ErbB2 helix heterodimer and EphA1 receptor homodimer. The ErbB1 and ErbB2 receptors (also known as EGFR/HER1 and HER2/Neu, respectively) as well as EphA1 are important for cell migration and are anticancer targets. Both TM dimer structures - the PDB identifiers are 2KS1²⁵ and 2K1L²⁶, respectively- have been solved by the Arseniev laboratory using solution NMR with the peptides embedded in dimyristoylphosphatidylcholine (DMPC)/dihexanoyl-phosphatidylcholine (DHPC) bicelles.

The TM segments of both proteins contain sequence motifs involved in TM helix association in other systems. Specifically, GXXXG motifs (where X is any amino acid and Gly may be replaced by other small amino acids such as Ala, Ser, Thr) occur at TM helix dimer interfaces²⁷. These residues are thought to stabilize helices by forming CH_a to mainchain carbonyl hydrogen bonds²⁸ and by minimizing the interactions with lipids. A tight packing of protein-protein contacts also shields polar mainchain and Ser/Thr sidechain OH groups⁸. Importantly, there are several GXXXG-like motifs in ErbB1/B2 and EphA1 dimers that could be employed for the helix-helix interactions and for switching between alternate states²⁹. There is experimental and computational evidence for alternative structures for the TM regions of the receptor tyrosine kinase superfamily in general^{30,31,32}. For example, left-handed ErbB1 homodimers are found in simulations³³ and a left-handed structure was also inferred for a homologous receptor, the ErbB3 homodimer, from NMR measurements³⁴. For the Eph family, the EphA1 TM dimer may also sample a left-handed helix dimer conformation (+15 degree crossing angle) that has indeed been observed in the similarly derived NMR structure of a homologue, EphA2³⁵. However, despite several proposed models (e.g. ^{36,37}), no detailed structure has been derived from experimental data for the alternative and presumed inactive conformation of the ErbB2 homodimer, or of ErbB1/B2 and EphA1. Thus, understanding the conformational behavior of the TM helix dimers in the simulations could provide considerable insight into the transmembrane signaling mechanism of these receptor tyrosine kinases.

This paper reports four all-atom microsecond simulations of ErbB1/B2 and EphA1 TM regions in DMPC bilayers. The first two were initialized with the NMR-derived structures of each helix dimer. The trajectories were generated with the C22/CMAP CHARMM protein forcefield and the relatively recently revised lipid forcefield, C36³⁸, and were run with CHARMM (approximately the first 100 ns) and then on the Anton supercomputer (last microsecond). Thus, they provide tests of the force field and of the comparability of the simulation programs and platforms. Because the structures are closely maintained, they also validate the NMR structures, an important finding since these structures were derived with a modest number of interhelical NOEs and no explicit helix-crossing or orientational restraints. Initial structures for the next two simulations were predicted using a Generalized Born/Replica Exchange protocol. Despite the known limitations of this implicit membrane model, its computational efficiency makes it an attractive method for constructing the initial configuration for more detailed simulations; however the deficiencies had not been reported in detail. We find the structures differed substantially from the configurations of the helices in the NMR structures, both when these structures were predicted and when the simulations were started with the NMR derived structures. It is shown, however, that microsecond explicit simulations can refine initially imperfect models, and also explore alternative contact patterns. A possible biological role for the alternate structures is considered.

METHODS

Peptides and notations

The peptide sequences of the NMR structures were used in each case. For the ErbB1/B2 heterodimer (2KS1) helix B1 refers to peptide EGCPTNGPKPSIATGMVGALLLLVVALGIGLFMRRRHIVRK and helix B2 refers to GCPAEQRASPLTSIISAVVGILLVVVLGVVFGILIKRRQQKIRK

For the EphA1 homodimer (2K1L) the sequence SPPVSRLTGGEIVAVIFGLLGAAALLGILVFRSRRA represents both helix A1a and A1b.

For brevity, the four primary systems are denoted Erb-nmr, Erb-md, Eph-nmr, and Eph-md. The first two indicate DMPC bilayers with ErbB1/B2 generated from the NMR and implicit MD simulation based models, respectively; the second similarly denote DMPC bilayers with EphA1. The peptide structures at t=0 for each simulation are labeled by the suffix “0”; e.g., Erb-md0. Erb-md0 is not identical, but is very close to the final structure obtained from the MD simulation that utilized replica exchange/implicit solvation because it was equilibrated in an explicit bilayer.

Simulation details

Unless otherwise noted, simulations were carried out using CHARMM (version C36a4r1)³⁸. Four of the all-atom simulations were continued on Anton, a supercomputer optimized for MD simulations³⁹, with closely similar run parameters (see details below). In all cases, the PARAM22 force field (FF) and CMAP correction⁴⁰ (also sometimes incorrectly referred to as C27) was used for the peptides; for the all-atom simulations, the lipids and water were described by the C36³⁸ and TIP3P parameter sets, respectively.

Replica-exchange (REX) simulations were carried out with the implicit solvent and lipid model of Im et al.²³ to predict initial TM dimer structures. The implicit lipid membrane spans the range of -15 to 15 Å in the z-direction but is unlimited in the x-y direction. To set up the calculations, the NMR derived structures for ErbB1/B2 (2KS1) and EphA1 (2K1L) TM dimers were aligned along the z-axis and translated to locate their centers of mass at z=0. The two helices were then separated in the x-y plane by an additional distance so that none of the peptide atoms between the helices are closer than 9 Å. As prescribed in the REX protocol²³, the simulations were run for 20 ns at 24 different temperatures, ranging from 323 to 695 K, with the target temperature set at 323 K.

The final structures from these REX simulations were inserted into explicit DMPC lipid bilayers (72 lipids/leaflet) using CHARMM-GUI⁴¹, and a target area per lipid of 60.6 Å². (DMPC forms the planar region of the DMPC/DHPC bicelle used experimentally.) TIP3P water molecules were added using CHARMM-GUI to yield a thickness (uniform above and below the bilayer) of no less than 15 Å above and below the farthest protein atom. Sodium and chloride ions were added to achieve neutral systems with near physiological ion concentration of 150 mM. The NMR based structures were similarly inserted into DMPC bilayers to yield a total of 4 systems. Trajectories of the four systems were then generated in the NPAT ensemble with constant particle number N, normal pressure P = 1 atm, the total surface area, A, obtained from the CHARMM-GUI procedure, and temperature T = 303 K (where pure DMPC is in fluid phase), and periodic boundary conditions. Electrostatic interactions utilized Particle Mesh Ewald with a real space cutoff of 12 Å, the same cutoff used for Lennard-Jones interactions. The SHAKE algorithm was applied to control the lengths of all bonds involving hydrogens and the integration time step was 2 fs. Using the CHARMM-GUI program, all systems were initially equilibrated for 300 ps before production runs.

Simulations of ErbB1/B2 and EphA1 initialized with the NMR structures (Erb-nmr and Eph-nmr) were carried out with CHARMM for 74 and 82 ns respectively; Erb-md and Eph-md were run to 150 ns for both dimers. Since some quantities such as helix crossing and tilting were still increasing monotonically near the end of these latter simulations, it was evident that convergence was not established and all four trajectories were continued on Anton for 1.0 μs.

Additional Test Simulations

This subsection summarizes the results of three sets of relatively short simulations that were useful for designing the longer simulations and for understanding their results.

First, ErbB1/B2 and EphA1 helices were inserted into a hydrated all atom-DMPC lipid bilayer at a separation so that none of the peptide atoms between the helices are closer than 9 Å. After 26 ns, neither of the helices showed a significant translational movement towards each other in the lipid bilayer (a required prelude to dimer formation), although relative rotations (ca. 30°) of the helices were observed. This result shows that single all-atom simulations on a timescale of tens of ns are of little utility for predicting helix dimer formation.

Simulations of ErbB1/B2 using the NMR structure for initial coordinates were carried out using the REX protocol described above. The helices moved away from the experimentally determined structure to substantially increase their contact area.

Lastly, 110–160 ns all-atom simulations of ErbB1/B2 and EphA1 helices were generated in DPPC and DLPC+POPC lipid bilayers to examine the effect of different lipids on the tilt and crossing angle. While these simulations are too short for definitive conclusions, taken as a group they support the notion that helices cross rather than tilt together in the explicitly represented bilayer.

Analysis

Procedures for calculating helix tilts, bends, relative rotations and crossing angles are described in the Supporting Information and in Fig. S1 a-d.

Root mean squared deviations (RMSD) (following C α superposition of whole or parts of the TM regions) and atom–atom distance calculations are standard. For contact maps, distances between residue pairs were calculated based on positions of the backbone C α on residues on helix A with those on helix B. For this distances map, coordinate frames (saved every 0.2 ns) were averaged over the last 50 ns of the trajectory.

The BMRB (Biological Magnetic Resonance Data Bank) deposited restraint file was used for ErbB1/B2 and one supplied for EphA1 by Bocharov and Arseniev was used to measure whether distances indicated by tertiary NOEs are satisfied over the course of the simulations. Note that none of the simulations reported here used these (or any other) distances (or angles) as restraints. In the case of the EphA1, restraints were converted from a united atom representation to approximate heavy atom positions by subtraction of 0.8 Å from the restraint. The distance between the nearest heavy atoms was then calculated.

RESULTS

General Features

Fig. 1 summarizes one of the essential results of the study: Simulations of TM dimers initiated with the experimentally based NMR structure (denoted –nmr) remain in that structure for over a microsecond (Fig. 1 left). Those initiated with the final conformation from REX MD simulations (which used an implicit lipid bilayer and solvation model and are denoted -md) differed substantially from the NMR derived structure at t=0 (Fig. 1 middle), but partially annealed to the experimental structure after a microsecond of refinement in explicit bilayer and water (right). Figure S2 shows a snapshot of the ErbB1/B2 TM dimer in explicit DMPC lipid bilayer after 50 ns of the all atom CHARMM simulation.

As anticipated from Fig. 1, and evident in Fig. S3, the RMSD of Erb-nmr and Eph-nmr from the NMR derived starting structures are very small (< 1.5 Å) in the contact region. The helix termini show considerable fluctuations, reflected in the large RMSD when calculated for the entire structure. The contact region RMSD for Erb-md and Eph-md are considerably larger, indicating significant differences with the NMR derived structures. However, while Erb-md remains distant (> 3.5 Å rms), Eph-md approaches the experimental structure to within 2.5 Å on several occasions (~160 ns and 400 ns), but then appears to settle into an alternative minimum ~ 4 Å away.

Helix Crossing, Tilt, and Rotation

Fig. 2 shows helix crossing angles: The helices of ErbB1/B2 (Erb-md0) and EphA1 (Eph-md0) from the replica-exchange implicit solvent simulations are almost parallel (cf. Fig. 1, middle panel), corresponding to initial crossing angles near zero in Fig. 2c,d. This is in marked contrast to the approximately 45° crossing angles of the NMR derived structures (shaded grey regions in Fig. 2a–d), and indicates a deficiency in the implicit model used to generate these conformations. As noted in Methods (Additional Test Simulations), incorrect results were also obtained from simulations carried out with the implicit model starting with the NMR structures.

Turning to the all-atom simulations in more detail, for both predicted structures the crossing angles increase during the first 100 ns to close to the NMR values, and then continue to increase for Erb-md (Fig. 2c), while remaining relatively constant for Eph-md (Fig. 2d) over the last part of the μs simulations. Erb-md and Eph-md also develop helix crossing in other lipid bilayers (Fig. S6). Crossing angles of Erb-nmr (Fig. 2a) and Eph-nmr (Fig. 2b) were maintained, though fluctuations are larger for the former. The tilt angles of helices are shown in the Fig. S4. Common tilting of the dimer relative to the explicit bilayer is modest in all cases ($\pm 30^\circ$ at most, see Fig. S5).

The lower panels of Fig. 2 show the relative orientation of the helices over the course of the simulations (see Fig. S1d for definitions). These are well preserved for Erb-nmr and Eph-nmr (Fig. 2e and f). In contrast, it is evident that the helices in the structures predicted with the implicit model are incorrectly oriented: helix B2 of Erb-md0 is rotated by 150–160° relative to the NMR derived structure (Fig. 2g), and both helices of Eph-md0 are rotated 50° (Fig. 2h). The helix rotations remain relatively constant for Erb-md over the course of the simulations, but the helices of Eph-md rotate after approximately 400 ns in a concerted fashion to values far from- and close to the NMR structure (helices A1a and A1b, respectively). These results indicate that the minima and alternative minima are rather deep in the energy landscape with respect to helix-helix contacts and rotations.

Helix kinks/bending and twisting

Helix kinking/bending and twisting are observed in some of the published structures of membrane helices and may be of biological importance^{42,43}. However, the great majority of NMR structures for TM helical peptides are refined with tight restraints that make helices regular (indicated by strong hydrogen bonding protecting amides against exchange, consistent chemical shift perturbations). Thus, distortions of the helices may be regarded as an exception, rather than the rule.

Helix bending is small (typically < 20°) in the NMR and REX derived structures for ErbB1/B2 and EphA1, and does not significantly develop during the course of the simulations (Fig. S7). Fluctuation values as high at 40° are observed during the first 800 ns of the simulations, but the curvatures are reduced to 10–15° by the last several hundred ns for all four helices.

Helices can distort by twisting, as shown in Fig. 3. In the NMR derived structures (left) the helices are formed as regular structures, so that there is a slight clockwise rotation of residue sidechains on successive turns, looking from the N-terminus. This pattern is maintained throughout the –nmr simulations. In the implicit MD derived structure this pattern can be badly disrupted. In fact, part of the ErbB2 helix even twists in anti-clockwise manner. The MD refinement corrects the majority of these distortions, also for Eph-md0 shown as a time-course for several examples in Fig. S8a and S8b. However, major transitions in the direction of untwisting occur up to 700 ns into the μ s long simulations.

The final structure of helix B2 from Erb-md still shows considerable twisting; while the C-terminal half of ErbB2 (no longer in contact with helix B1) is close to the NMR derived structure, the N-terminus is still slightly under-rotated from residue 11 right through the contact region to residue 36 (Fig. 3, top right). Interestingly, this is also the helix that is misaligned in the structure by a helix rotation of 140° (Fig. 2g), suggesting that the alternate contacts are formed by a sidechain alignment at the expense of mainchain regularity. By contrast helix B1 has a similar helical pitch as the NMR derived structure (not shown). Helix A1a of Eph-md (Fig. 3, bottom right) shows a slight under-twisting ($\sim 30^\circ$) at the N-terminus and an over-twisting ($\sim 30^\circ$) at the C-terminus (which is four turns from the area of closest helix-helix contact). In terms of twisting, the helix A1b is in close agreement with the NMR derived structure (not shown).

Proximity to NMR derived structures

The NMR derived tertiary structures of ErbB1/B2 and EphA1 rely on a collection of 13 and 15 inter-helix distance restraints (NOEs), respectively^{25,26}. Representative NOE distances are shown in Fig. S9. The great majority of these distances are satisfied throughout the trajectory for Erb-nmr and Eph-nmr. A different picture emerges from Erb-md and Eph-md: Even though one helix presents the correct surface as shown in the helix rotation analysis (Fig. 2) and in contact maps (discussed below), this does not lead to close residue interaction distances that would correspond to those seen experimentally.

Distance map and contact residue comparisons

As shown in Fig. S3, the RMSD in the contact regions are small for Erb-nmr and Eph-nmr, but larger for Erb-md and Eph-md. This is consistent with the observation that the Eph-nmr and Erb-nmr contact maps closely overlap with those of the NMR derived reference structures, but that only partial overlap is seen for Eph-md and Erb-md (Fig. 4). Specifically in these latter maps there is good overlap for contacts with one of the helices. By contrast, the second helix, helix B2 of the Erb dimer, is displaced, making fewer contacts. In the case of EphA1 one helix is displaced towards the C-terminal end of the other. The similarity and differences are most easily illustrated by molecular graphics images of both systems at the contact region (Figs. 5 and 6).

Contact details for ErbB1/B2 dimer: In ErbB1 there is an N-terminal double/overlapping GXXXG-like motif, ¹⁵TGXXG²⁰A (i.e. TXXXG and GXXXA) and a C-terminal ²⁷SXXX³¹A motif. ErbB2 has an N-terminal glycine zipper ¹²TXXX¹⁶SXXX²⁰G with an overlapping ¹³SXXX¹⁷A motif, and a C-terminal ²⁷GXXX³¹G segment. In the NMR derived structure only the N-terminal motifs are involved in dimer formation²⁵. This is found for both Erb-nmr and Erb-md because none of the C-terminal motifs are close enough to interact. The ¹⁵TGXXG²⁰A motif in ErbB1 is the region of closest contact of this helix (with the small sidechain residues facing ErbB2 as shown in Fig. 5). The second helix in the dimer, ErbB2, is rotated and engages ¹³SXXX¹⁷A, as an alternative to its ¹²TXXX¹⁶SXXX²⁰A motif seen in the NMR derived structure (cyan vs. green contacts). This alternate packing also explains why the helix crossing angle is larger than in the NMR

structure. On both helices, residues I13 in ErbB2 and I14 in ErbB1 block a smaller crossing angle. In fact the crossing angle is close to 90° and in order to prevent mismatching on the C-terminal side of the membrane bilayer, a kink is introduced in ErbB2 just after the area of contact. Thus, from packing considerations, the contact area (and rotated ErbB2 helix) leads to a reasonable and stable structure.

Contact details for EphA1 dimer: In the EphA1 there are dimerization motifs $^{15}\text{AXXX}^{19}\text{GXXX}^{23}\text{G}$ in the center and additional motifs $^7\text{GXXXG}^{11}$ at the N- and $^{25}\text{AXXX}^{29}\text{G}$ near the C-terminus²⁶. The NMR structure shows that only the middle motif is utilized and this is also true in all of the simulations. EphA1 helices start at residue G11 and E12 for helix A1a and A1b in Eph-nmr, but at residue V14 for the A1a helix and E12 for the A1b helix in Eph-md. Interestingly, the experimental NMR paper suggested that the charge on E12 at high pH leads to a fractional unfolding in the same region of the helix²⁶. By contrast helix A1a has a similar length to the reference structure, possibly because E12 is neutralized by interactions with R6 (of helix A1b). In part due to the increased crossing angle, helix A1a is shifted in its contacts with helix A1b towards the C-terminus of the latter; thus, for example, the prominent contact of A15 (in helix A1a) is not made with the equivalent residue in helix A1b, but instead A15 contacts G19 and G23. Overall, then, the final Eph-md structure can be rationalized as having the same $^{15}\text{AXXX}^{19}\text{GXXX}^{23}\text{G}$ motif that is involved in the Eph-nmr0 structure, but in a manner that has compressed the interactions in helix A1a due to a larger crossing angle with helix A1b. The structure may also be consistent with the pH-dependent changes seen in the NMR spectra, which propagate from E12 to G23²⁶. It could, therefore, represent an alternate state of the EphA1 TM helix dimer.

Hydrogen bonds, Contacts at the N- and C-termini

The interhelical NMR NOE restraints are between sidechain methyl groups, as these are adequately resolved in the spectra and come close to one another. However, another type of contact that was inferred for the structure of ErbB2/B1 is CH α – oxygen bonding. Such hydrogen bonds are generally weak, but are thought to play a significant role in membrane proteins³⁹. There is no specific hydrogen bond term in the CHARMM potential function, but for NH – O=C hydrogen bonds, the geometry and distance of hydrogen bonds are well reproduced from the VDW and electrostatic potential alone⁴⁴. Bringing the mainchain of the helices close is a mechanism for shielding the polar peptide and sidechain Ser/Thr groups from lipids, and in the Erb-nmr simulation several interhelix CH α – oxygen hydrogen bonds were observed, involving Gly, Ala and Ser residues. Six such hydrogen bonds are maintained over the course of the Erb-md trajectory but only 3 such mainchain or sidechain groups are occasionally close in the Erb-md simulation (See Fig. S10a,b for details). In the EphA1 NMR derived structure, there are two inter helix H α – mainchain oxygen hydrogen bonds are maintained throughout the Eph-nmr trajectory (Fig. S10c). Although several CH α – O=C hydrogen bonds are formed, the ones finally refined for the predicted started simulation of EphA1 are different from the ones seen in the NMR structure.

Contacts are not confined to the helical regions and it is known that TM flanking regions can influence the structure of the helices⁵. All simulations show contacts near to the peptide N-termini (see Fig. 4), although these contacts differ in detail. Differences are already between the NMR structure started simulation and the NMR reference structure, showing that this region is flexible and/or that alternative structures are sampled (details are shown in Fig. S11).

Erb-md and Eph-md trajectories show that the N-terminal regions form many additional contacts (see Fig. 4 and details in Fig. S11b).

DISCUSSION

A satisfactory search of conformational space using all-atom representations of peptides in membranes is still on the edge, if not beyond of computational feasibility. Restraints can narrow the search, but experimentally or homology-derived restraints may not be available or be necessarily accurate. Instead, a popular option is to simplify the representation, e.g. by coarse graining¹² or, as done here, by an implicit representation of lipid and solvent²³. This lowers the calculation cost by two to three orders of magnitude. However, the study presented here demonstrates several shortcomings of an implicit representation/replica exchange protocol when used in absence of restraints, some of which have already been reported²⁴. As the helices associate features of their regular geometry are compromised, for example leading to helix twisting. These distortions are introduced even when the helices are associated with the surfaces in the orientation that corresponds to the NMR derived structures. Since these NMR derived structures are very stable in the all-atom simulations, distortions must arise due to the implicit model, aided by the higher simulation temperatures in replica exchange.

The implicit model fails to maintain the NMR derived structure and also could not locate a reasonable “crossed” geometry. However, this could serve as a useful starting point to make improvements to the model; the simulation parameters favor structures with large contacts between the helices, indicating an imbalance of the attraction between peptide sidechains and the (implicit) attraction of sidechains to lipids. While a positive surface tension in the aqueous region accounts for the hydrophobic effect, similarly, a negative surface tension term in the bilayer region (i.e. increasing the area exposed to lipids, lowers the energy) would stabilize crossed configurations relative to those in maximal contact.

Our study suggests that several alternative/enhanced protocols for the prediction of TM helix dimers should be considered. a) a harmonic restraint could be applied to keep helix geometry regular. This is already done in most protocols employing coarse-grained force fields¹². However, given the possible importance of TM helix kinking/bending and twisting in biological function^{43,45} such restraints should be mild. b) High temperature replica exchange could be replaced with umbrella sampling, currently developed for single TM helices^{6,7}. Overall, the results also suggest that the more accurate all atom force fields should be used throughout the search and refinement stage, as improved implicit solvation protocols are being developed.

The present paper furthermore provides important information on the NMR derived structures for two important systems, as well as for the utility of the all-atom CHARMM force field³⁸ (containing new parameters for lipids) for structure refinement: The NMR derived helix dimers are closely maintained with respect to their starting structures over a μ s long trajectory. This in itself is remarkable, as the structures were derived with a modest number of tertiary restraints (i.e. interhelix NOEs), compared to the number of such restraints typically available for globular proteins. However, the NOEs were evaluated extensively, also with reference to relaxation calculations on the structural models²⁶. The NMR derived structures were not refined with solvent or a membrane potential; no restraints are directly responsible for the helix crossing angle. Thus, the helix crossing angles in the NMR structures, closely reproduced in the Erb- and Eph-nmr μ s simulations, largely arise from packing considerations. Fluctuations of helix crossing and tilting are modest in the simulations implying that the structures are in a deep energy minimum. By contrast, fluctuations are greater in the structures derived from the sampling in the implicit model, suggesting that the minimum for the alternate structures may be more shallow. Future calculations will explore the depth of these minima and possible pathways between them, but these calculations are beyond the scope of this report.

The refinement procedure works to the extent that the majority of helix twists are eliminated. Furthermore the protein-protein and protein-lipid interaction appear to be better balanced. Helix dissociation/association has recently been measured to occur on a timescale of 50 ms for the weakly bound ErbB4 system⁴⁶. However, the timescale of helix motions in membranes, such as translational and rotational diffusion of individual helices or helices within dimers has been reported on the order of 1–100 μ s^{47,48}. This is slower than could be sampled here, although at least one large transition is seen for the orientation of one of the helices in each system (Fig. 3). The timescale needed for the refinements seen is larger than would be useful in routine applications, although with the continuing increase in CPU, and also GPU speed, μ s timescale simulations are now becoming more common.

An important observation concerns the differences in the contact regions of the simulation refined implicit- and the experimentally-derived structures. Although overall similar segments of the peptides associate, compared to those of the NMR derived structures, the residues that are in close contact are only partly the same. Specifically, in each of the simulation-derived ErbB1/B2 and EphA1 dimers one of the two helices is rotated relative to the experimentally determined structure. This means residues that make contacts in the NMR derived structures are involved on one of the helices but not on the other, breaking the symmetry in case of EphA1. The stability of these alternate structures, relative to the NMR derived configuration, implies that general features of the contact regions already appear to be sufficient for dimerization in the particular peptide segment.

The alternate structures are intriguing from a biological perspective:

Firstly, for these specific systems, a helix-dimer rotational mechanism has been implicated in the regulation of receptor activity: Bell et al⁴⁹ investigated the rotational linkage of the ErbB2 transmembrane domain to the kinase domain, and proposed that a correct rotational conformation of surface residues is required for receptor tyrosine kinases dimerization and activation. Dimerization of the helices itself is not sufficient, but it is also required that the orientations of the helices, intra and extracellular regions are correct to stimulate activity^{31,32}. For both ErbB1/B2 and EphA1 helix dimers, we observed significant helix rotations during the simulation. In the case of EphA1 the correspondence with the NMR derived structure was close before the structure fell into an alternate minimum that is similar to that of the ErbB1/B2 alternate structure, in terms of helix rotation.

Secondly, it can be argued that large changes in crossing angle or piston-like movement of helices are not good mechanisms for signal transduction as they would involve high energy states where a considerable hydrophobic mismatch occurs. Having polar groups surround a charged residue such as Glu12 in EphA1 is critical in this respect, because this sidechain is at the boundary of the charged and hydrophobic lipid groups. The sidechain is completely negatively charged in the simulations, whereas in the cell, the pKa may be increased so that immersion of the residue into the bilayer is allowed⁵⁰ as an uncharged species, provided it is surrounded by other polar groups, such as Ser/Thr sidechains. The charged residue Glu12 is unique to EphA1 (no other Eph family member TM domains have this). Ser/Thr residues close to the N-terminus in ErbB1/B2 also penetrate the membrane bilayer deeply. On the other side, at the C-termini of both systems, a number of Arg, Lys (and in the case of ErbB1 an additional His) forms a positively charged plug that is often seen in TM helices, limiting the immersion depth⁵¹. This would make a piston mechanism an unlikely one for cell signaling across the membrane in these TM receptors, unless these movements are rather small, for example ~ 1.5 Å, as seen in certain bacterial chemoreceptors⁵². Rotation around the helices would have a much smaller effect on hydrophobic matching, except when the helices have a large tilt in the membrane. Subtle changes in helix-helix orientation (< 90°) are unlikely to lead to a regulatory mechanism. If these stipulations are correct, a possible

alternative mechanism would be helix rotation and, it would not be surprising to see rotation differences of 140°, as observed here for one of the helices in each system.

Thirdly, while the NMR derived structures for ErbB1/B2 and EphA1 were proposed as the active configuration of the TM helix dimer^{25,26}, the alternate, and thus possibly inactive configurations have an intriguing feature: One of the helices occludes a contact area that is similar to the NMR derived structure, while the second helix has the same area exposed and thus available to form another helix-helix contact. By contrast to a rotation of both helices by 180°, which would expose two new contact areas (prone to aggregation/ polymer formation), the rotation of one helix by 120° exposes a contact area that is already known to be employed in helix-helix contacts. By association with additional helix pairs at an angle of ca. 120°, the protein could form a hexamer circle. Several membrane proteins (both as active and inactive forms) have already been characterized in hexamer or pentamer configuration^{53,54}. In the case of the RTK family, a non-symmetrical dimer of the intracellular kinase domain region is regarded as the active form, but other inactive dimeric forms have also been reported⁵⁵. In case of a hexamer or pentamer, stabilized through TM helices, the intracellular regions are likely to be too crowded for catalytic activity. The extracellular regions of the receptor would also be in close proximity. These distances would be increased and the TM hexamer/pentamer would be disrupted upon binding of protein ligand, thus contributing to a mechanism of activation (e.g. formation of NMR-structure like TM dimers). The above mechanism is speculation at this point, but it may help to stimulate experiments to either support or to disprove such a model.

CONCLUSIONS

Structures of TM ErbB1/B2 heterodimers and EphA1 homodimers are well maintained in 1 μs explicit simulations when initialized with the experimentally derived NMR structures, thus further validating the structures, the CHARMM force field and the simulation protocols on Anton. The great majority of tertiary (NOE) NMR restraints are satisfied in these unrestrained simulations. Structures predicted for the TM helix dimers from a replica exchange protocol using an implicit representation of lipids and solvent tend to maximize the contact area between the helices at the expense of helix regularity. Microsecond trajectories started with these structures initially show large fluctuations that, however, serve to remedy many of the unrealistic features (e.g. by creating more regular helices) and come close to the experimental structures. However, these lengthy simulations indicate that barriers for inter-conversion of the alternate and NMR derived structures are high. Overall, the study suggests avenues for future improvements in TM dimer structure prediction that combines restraints, explicit representation and enhanced sampling algorithms. The stability of the alternate structures could be rationalized by GXXXG-like motifs and other key interactions. Finally, we hypothesize that the alternate restructures may have a biological role in the formation of inactive receptor clusters.

Supplementary Material

Refer to Web version on PubMed Central for supplementary material.

Acknowledgments

This research was initiated with an ARRA supplement to NIH grant R01GM073071 and continued with partial support of 1R01GM092851 (MB), and by the Intramural Research Program of the NIH, National Heart, Lung and Blood Institute (RWP, RMV, and AJS). Some of the dynamics calculations and analyses were carried out at the Case Western Reserve High Performance Cluster. The study was also supported through Teragrid grant of TG-MCB070074N. The use of Anton at the Pittsburg Supercomputer Center was supported by award MCB110023P through NIH award RC2GM093307 to CMU. We thank Myriam Cotten for a critical reading of the manuscript.

REFERENCES

1. Cymer F, Schneider D. Transmembrane helix-helix interactions involved in ErbB receptor signaling. *Cell Adhesion Migration*. 2010; 4:299–312. [PubMed: 20212358]
2. Stansfeld PJ, Sansom MS. Molecular simulation approaches to membrane proteins. *Structure*. 2011; 19:1562–1572. [PubMed: 22078556]
3. Braun R, Engelman DM, Schulten K. Molecular Dynamics Simulations of Micelle Formation around Dimeric Glycophorin A Transmembrane Helices. *Biophys J*. 2004; 87:754–763. [PubMed: 15298884]
4. Petracche HI, Grossfield A, MacKenzie KR, Engelman DM, Woolf TB. Modulation of glycophorin A transmembrane helix interactions by lipid bilayers: molecular dynamics calculations. *J. Mol. Biol.* 2000; 302:727–746. [PubMed: 10986130]
5. Zhang J, Lazaridis T. Transmembrane helix association affinity can be modulated by flanking and noninterfacial residues. *Biophysical Journal*. 2009; 96:4418–4427. [PubMed: 19486666]
6. Kim T, W Im. Revisiting hydrophobic mismatch with free energy simulation studies of transmembrane helix tilt and rotation. *Biophysical Journal*. 2010; 99:175–183. [PubMed: 20655845]
7. Frank A, Andricioaei I. A comparative study on the ability of two implicit solvent lipid models to predict transmembrane helix tilt angles. *J Membrane Biol*. 2011; 239:57–62. [PubMed: 21152910]
8. Cymer F, Veerappan A, Schneider D. Transmembrane helix-helix interactions are modulated by the sequence context and by lipid bilayer properties. *Biochim Biophys Acta*. 2012; 1818:963–973. [PubMed: 21827736]
9. Rui H, Lee J, Im W. Comparative molecular dynamics simulation studies of protegrin-1 monomer and dimer in two different lipid bilayers. *Biophysical Journal*. 2009; 97:787–795. [PubMed: 19651037]
10. Henin J, Pohorille A, Chipot C. Insights into the recognition and association of transmembrane alpha-helices. The free energy of alpha-helix dimerization in glycophorin A. *JACS*. 2005; 127:8478–8484.
11. Cuthbertson JM, Bond PJ, Sansom MS. Transmembrane helix-helix interactions: comparative simulations of the glycophorin A dimer. *Biochemistry*. 2006; 45:14298–14310. [PubMed: 17128969]
12. Psachoulia E, Marshall DP, Sansom MS. Molecular dynamics simulations of the dimerization of transmembrane alpha-helices. *Accounts of Chemical Research*. 2010; 43:388–396. [PubMed: 20017540]
13. Pappu RV, Marshall GR, Ponder JW. A potential smoothing algorithm accurately predicts transmembrane helix packing. *Nature Structural Biology*. 1999; 6:50–55.
14. Sengupta D, Marrink SJ. Lipid-mediated interactions tune the association of glycophorin A helix and its disruptive mutants in membranes. *Phys Chem Chem Phys*. 2010; 12:12987–12996. [PubMed: 20733990]
15. Barth P, Schonbrun J, Baker D. Toward high-resolution prediction and design of transmembrane helical protein structures. *PNAS*. 2007; 104:15682–15687. [PubMed: 17905872]
16. Pellegrini-Calace M, Carotti A, Jones DT. Folding in lipid membranes (FILM): a novel method for the prediction of small membrane protein 3D structures. *Proteins*. 2003; 50:537–545. [PubMed: 12577259]
17. Li R, Gorelik R, Nanda V, Law PB, Lear JD, DeGrado WF, Bennett JS. Dimerization of the transmembrane domain of Integrin alphaIIb subunit in cell membranes. *The Journal of Biological Chemistry*. 2004; 279:26666–26673. [PubMed: 15067009]
18. Dell'Orco D, De Benedetti PG, Fanelli F. In silico screening of mutational effects on transmembrane helix dimerization: insights from rigid-body docking and molecular dynamics simulations. *J Phys Chem B*. 2007; 111:9114–9124. [PubMed: 17602582]
19. Samna SO, Garnier N, Genest M. Molecular dynamics simulation approach for the prediction of transmembrane helix-helix heterodimers assembly. *Eur Biophys J*. 2007; 36:1071–1082. [PubMed: 17646979]

20. Kokubo H, Okamoto Y. Prediction of membrane protein structures by replica-exchange Monte Carlo simulations: case of two helices. *Journal of Chemical Physics*. 2004; 120:10837–10847. [PubMed: 15268111]
21. Volynsky PE, Mineeva EA, Goncharuk MV, Ermolyuk YS, Arseniev AS, Efremov RG. Computer simulations and modeling-assisted ToxR screening in deciphering 3D structures of transmembrane alpha-helical dimers: ephrin receptor A1. *Phys Biol*. 2010; 7:16014. [PubMed: 20228445]
22. Lazaridis T. Effective energy function for proteins in lipid membranes. *Proteins*. 2003; 52(2):176–192. [PubMed: 12833542]
23. Im W, Feig M, Brooks CL. An implicit membrane generalized born theory for the study of structure, stability, and interactions of membrane proteins. *Biophysical Journal*. 2003; 85:2900–2918. [PubMed: 14581194]
24. Bu L, Im W, Brooks CL. Membrane assembly of simple helix homo-oligomers studied via molecular dynamics simulations. *Biophys J*. 2007; 92:854–863. [PubMed: 17085501]
25. Mineev KS, Bocharov EV, Pustovalova YE, Bocharova OV, Chupin VV, Arseniev AS. Spatial structure of the transmembrane domain heterodimer of ErbB1 and ErbB2 receptor tyrosine kinases. *J Mol Biol*. 2010; 400:231–243. [PubMed: 20471394]
26. Bocharov EV, Mayzel ML, Volynsky PE, Goncharuk MV, Ermolyuk YS, Schulga AA, Artemenko EO, Efremov RG, Arseniev AS. Spatial structure and pH-dependent conformational diversity of dimeric transmembrane domain of the receptor tyrosine kinase EphA1. *J Biol Chem*. 2008; 283:29385–29395. [PubMed: 18728013]
27. Russ WP, Engelman DM. The GxxxG motif: a framework for transmembrane helix-helix association. *J Mol Biol*. 2000; 296:911–919. [PubMed: 10677291]
28. Senes A, Ubarretxena-Belandia I, Engelman DM. The Calpha ---H...O hydrogen bond: a determinant of stability and specificity in transmembrane helix interactions. *Proc Natl Acad Sci U S A*. 2001; 98:9056–9061. [PubMed: 11481472]
29. Escher C, Cymer F, Schneider D. Two GxxxG-like motifs facilitate promiscuous interactions of the human ErbB transmembrane domains. *J Mol Biol*. 2009; 389:10–16. [PubMed: 19361517]
30. He L, Hoffmann AR, Serrano C, Hristova K, Wimley WC. High-throughput selection of transmembrane sequences that enhance receptor tyrosine kinase activation. *J Mol Biol*. 2011; 412:43–54. [PubMed: 21767549]
31. Yu X, Sharma KD, Takahashi T, Iwamoto R, Mekada E. Ligand-independent dimer formation of epidermal growth factor receptor (EGFR) is a step separable from ligand-induced EGFR signaling. *Mol Biol Cell*. 2002; 13:2547–2557. [PubMed: 12134089]
32. Moriki T, Maruyama H, Maruyama IN. Activation of preformed EGF receptor dimers by ligand-induced rotation of the transmembrane domain. *J Mol Biol*. 2001; 311:1011–1026. [PubMed: 11531336]
33. Prakash A, Janosi L, Doxastakis M. Self-association of models of transmembrane domains of ErbB receptors in a lipid bilayer. *Biophys J*. 2010; 99:3657–3665. [PubMed: 21112290]
34. Mineev KS, Khabibullina NF, Lyukmanova EN, Dolgikh DA, Kirpichnikov MP, Arseniev AS. Spatial structure and dimer--monomer equilibrium of the ErbB3 transmembrane domain in DPC micelles. *Biochim Biophys Acta*. 2011; 1808:2081–2088. [PubMed: 21575594]
35. Bocharov EV, Mayzel ML, Volynsky PE, Mineev KS, Tkach EN, Ermolyuk YS, Schulga AA, Efremov RG, Arseniev AS. Left-handed dimer of EphA2 transmembrane domain: Helix packing diversity among receptor tyrosine kinases. *Biophys J*. 2010; 98:881–889. [PubMed: 20197042]
36. Fleishman SJ, Schlessinger J, Ben-Tal N. A putative molecular-activation switch in the transmembrane domain of erbB2. *Proc Natl Acad Sci U S A*. 2002; 99:15937–15940. [PubMed: 12461170]
37. Beevers AJ, Damianoglou A, Oates J, Rodger A, Dixon AM. Sequence-dependent oligomerization of the Neu transmembrane domain suggests inhibition of "conformational switching" by an oncogenic mutant. *Biochemistry*. 2010; 49:2811–2820. [PubMed: 20180588]
38. Klauda JB, Venable RM, Freites JA, O'Connor JW, Tobias DJ, Mondragon-Ramirez C, Vorobyov I, MacKerell AD Jr, Pastor RW. Update of the CHARMM all-atom additive force field for lipids: validation on six lipid types. *J Phys Chem B*. 2010; 114:7830–7843. [PubMed: 20496934]

39. Dror RO, Jensen MØ, Shaw DE. Elucidating membrane protein function through long-timescale molecular dynamics simulation. *Conf Proc IEEE Eng Med Biol Soc.* 2009; 2009:2340–2342. [PubMed: 19965181]
40. Buck M, Bouquet-Bonnet S, Pastor RW, MacKerell AD Jr. Importance of the CMAP correction to the CHARMM22 protein force field: dynamics of hen lysozyme. *Biophys J.* 2006; 90:L36–L38. [PubMed: 16361340]
41. Jo S, Lim JB, Klauda JB, Im W. CHARMM-GUI Membrane Builder for mixed bilayers and its application to yeast membranes. *Biophys J.* 2009; 97:50–58. [PubMed: 19580743]
42. Li Y, Tamm LK. Structure and plasticity of the human immunodeficiency virus gp41 fusion domain in lipid micelles and bilayers. *Biophys J.* 2007; 93:876–885. [PubMed: 17513369]
43. Kim C, Schmidt T, Cho EG, Ye F, Ulmer TS, Ginsberg MH. Basic amino-acid side chains regulate transmembrane integrin signaling. *Nature.* 2012; 481:209–213.
44. Buck M, Karplus M. Hydrogen bond energetics: A simulation and statistical analysis of Nmethyl acetamide (NMA), water, and human lysozyme. *J.Phys.Chem. B.* 2001; 105:110000–111015.
45. Cao Z, Bowie JU. Shifting hydrogen bonds may produce flexible transmembrane helices. *Proc Natl Acad Sci U S A.* 2012; 109:8121–8126. [PubMed: 22566663]
46. Bocharov EV, Mineev KS, Goncharuk MV, Arseniev AS. Structural and thermodynamic insight into the process of “weak” dimerization of the ErbB4 transmembrane domain by solution NMR. *Biochimica et Biophysica Acta.* 2012; 1818:2158–2170. [PubMed: 22579757]
47. Jones DH, Barber KR, VanDerLoo EW, Grant CW. Epidermal growth factor receptor transmembrane domain: 2H NMR implications for orientation and motion in a bilayer environment. *Biochemistry.* 1998; 37:16780–16787. [PubMed: 9843449]
48. Sharpe S, Barber KR, Grant CW, Goodyear D, Morrow MR. Organization of model helical peptides in lipid bilayers: insight into the behavior of single-span protein transmembrane domains. *Biophys J.* 2002; 83:345–358. [PubMed: 12080125]
49. Bell CA, Tynan JA, Hart KC, Meyer AN, Robertson SC, Donoghue DJ. Rotational coupling of the transmembrane and kinase domains of the Neu receptor tyrosine kinase. *Mol Biol Cell.* 2000; 11:3589–3599. [PubMed: 11029057]
50. Barrera FN, Weerakkody D, Anderson M, Andreev OA, Reshetnyak YK, Engelman DM. Roles of carboxyl groups in the transmembrane insertion of peptides. *J Mol Biol.* 2011; 413:359–371. [PubMed: 21888917]
51. Yuzlenko O, Lazaridis T. Interactions between ionizable amino acid side chains at a lipid bilayer–water interface. *J Phys Chem B.* 2011; 115:13674–13684. [PubMed: 21985663]
52. Hall BA, Armitage JP, Sansom MS. Transmembrane helix dynamics of bacterial chemoreceptors supports a piston model of signalling. *PLoS Comput Biol.* 2011; 7:e1002204. [PubMed: 22028633]
53. Jenei ZA, Borthwick K, Zammit VA, Dixon AM. Self-association of transmembrane domain 2(TM2), but not TM1, in carnitine palmitoyltransferase 1A: role of GXXXG(A) motifs. *J Biol Chem.* 2009; 284:6988–6997. [PubMed: 19136561]
54. Kelly EM, Hou Z, Bossuyt J, Bers DM, Robia SL. Phospholamban oligomerization, quaternary structure, and sarco(endo)plasmic reticulum calcium ATPase binding measured by fluorescence resonance energy transfer in living cells. *J Biol Chem.* 2008; 283:12202–12211. [PubMed: 18287099]
54. Lemmon MA. Ligand-induced ErbB receptor dimerization. *Exp Cell Res.* 2009; 315:638–648. [PubMed: 19038249]

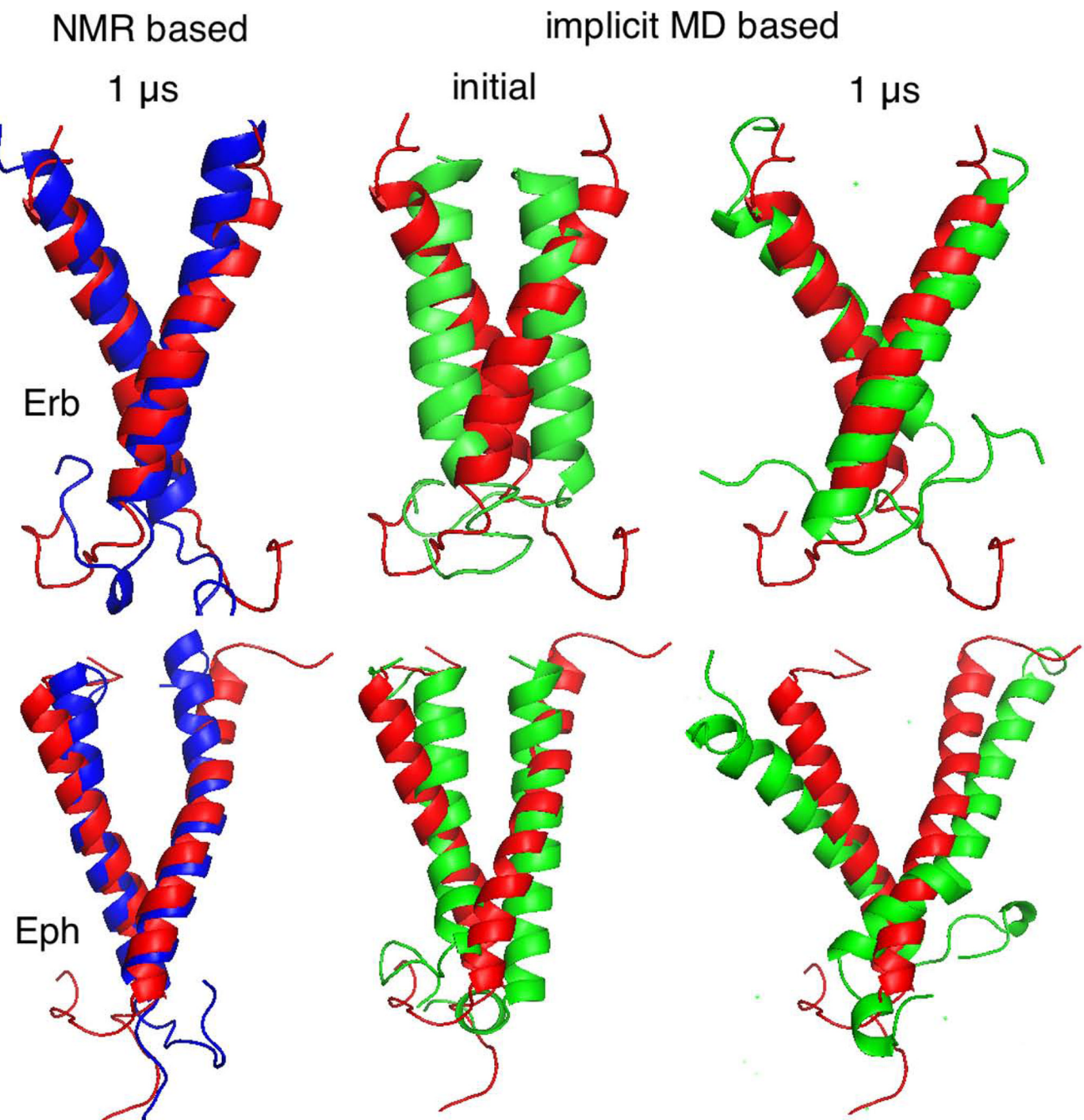
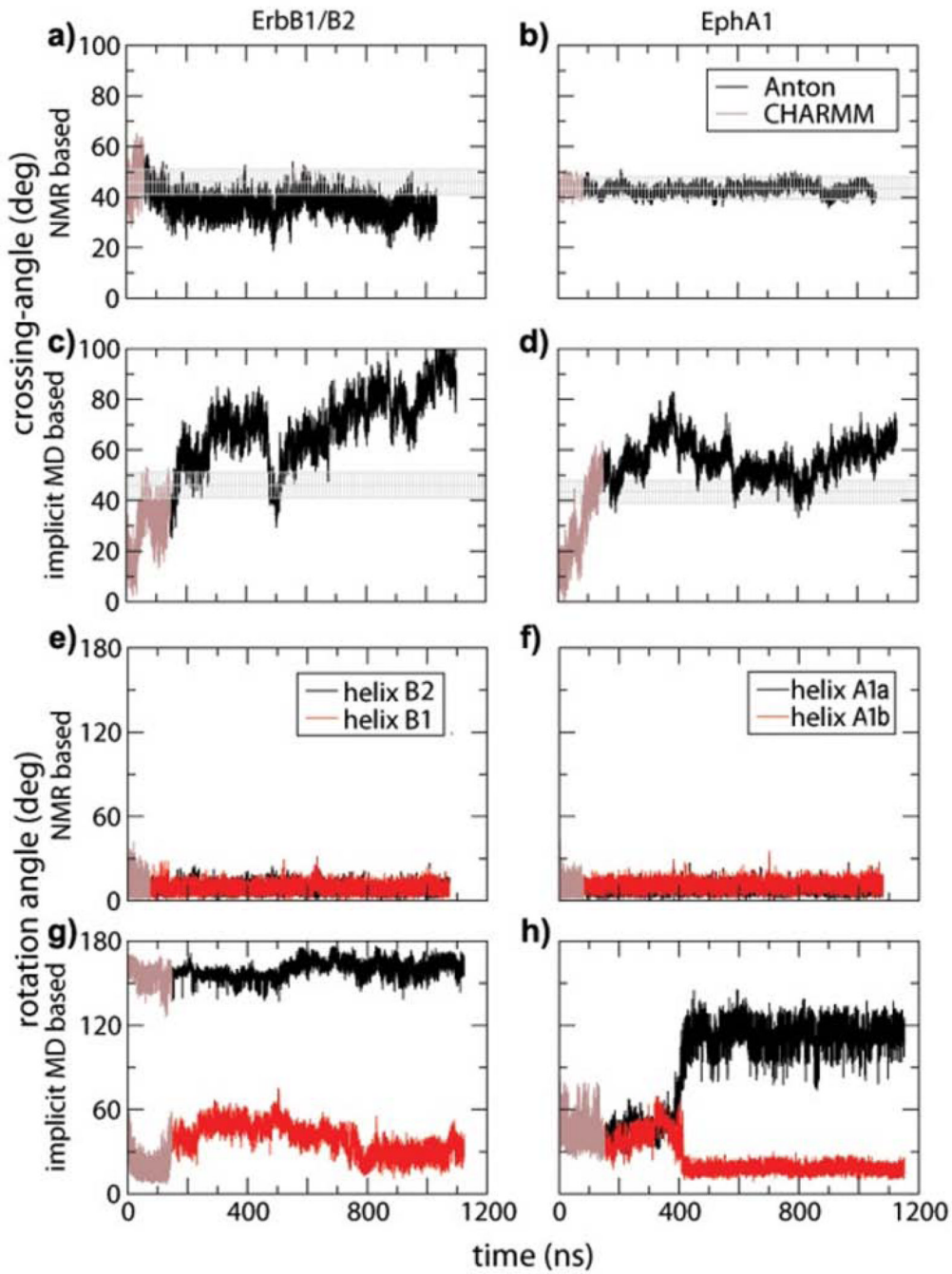


Figure 1.

Comparison of experimental NMR based (-nmr0, red) and simulated structures of ErbB1/B2 (top) and EphA1 (bottom). Structures from simulations initialized with the NMR structures are colored blue (-nmr); those from REX MD on an implicit bilayer model are green (-md).

**Figure 2.**

a-d) Crossing angles for transmembrane helices of ErbB1/B2 and EphA1, with experimental range denoted by shaded grey, and e-h) rotation of helices relative to the NMR derived structures.

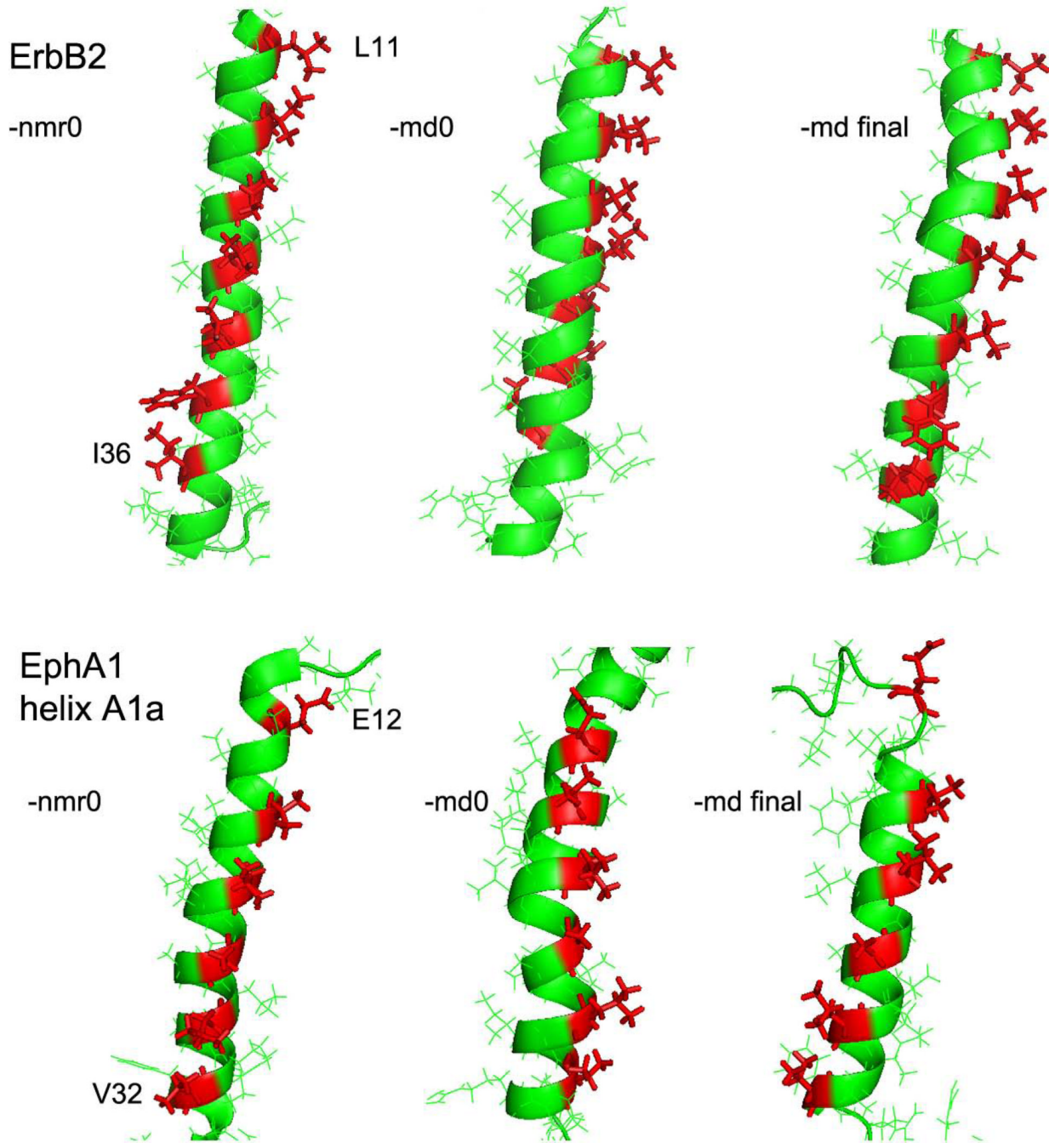
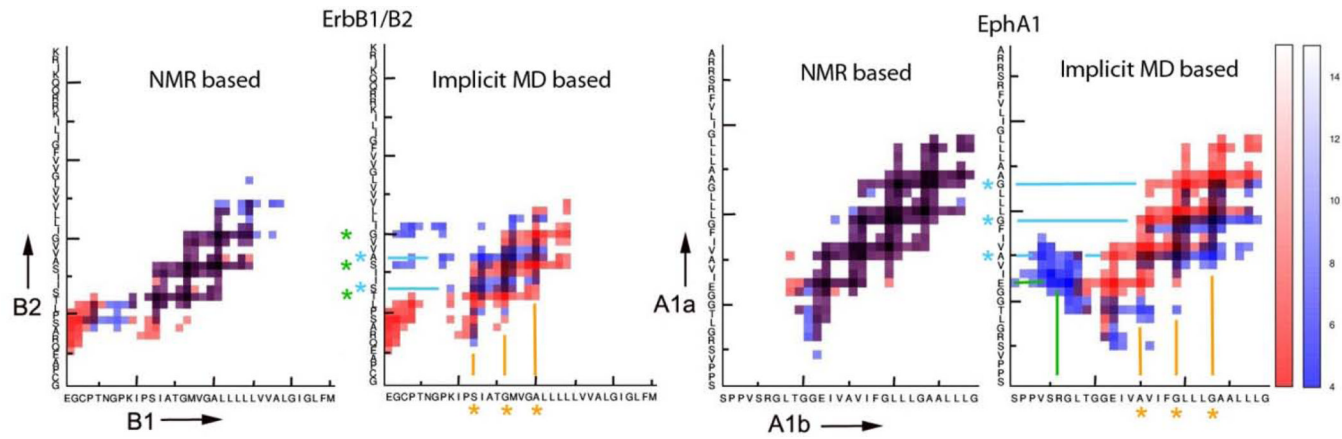


Figure 3.

Helix B2 from the ErbB1/B2 dimer (top) and helix A1 from the EphA1 dimer (bottom) with sidechains in stick representation (red) every 4 residues. NMR derived structures (left); implicit model derived structures at the start (middle) and end (right) of the all-atom MD simulations.

**Figure 4.**

Contact surface residue distance map for ErbB1/B2 (left) and EphA1 (right) comparing results from the simulations starting from NMR structures (blue) with the NMR derived structures themselves (red). Saturation of the color indicates Ca-Ca distance (right hand scale). Purple represents the overlap between red and blue. Sequences are shown for the helices (in direction of N- to C-terminus as indicated); short and long marks label 5 and 10 residue intervals. * indicates some of the GXXXG-like motifs discussed in the text and lines indicate the contacts formed in the simulations. In both -md simulations, one helix has residues in contact that are similar to those of the NMR derived structures (indicated by the vertical purple stripes showing overlap, highlighted by orange lines); This is the helix with the peptide sequence given on the horizontal axis. Alternate contacts utilized by the second helix are indicated in light blue.

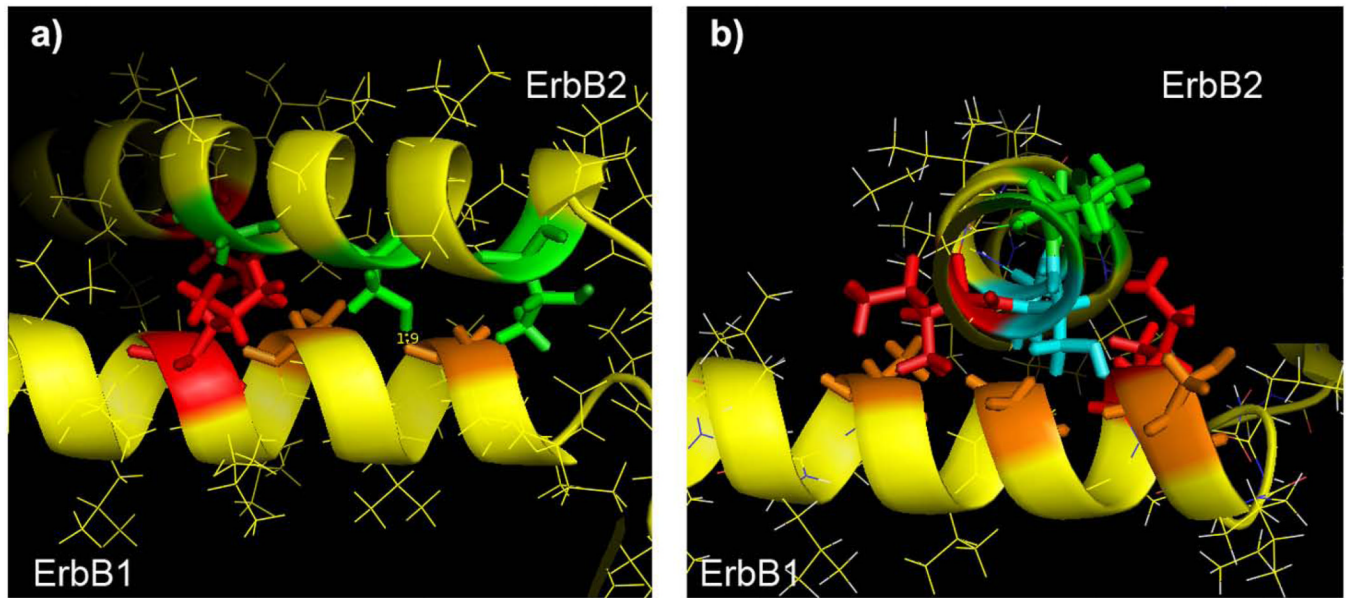


Figure 5.

Region of ErbB1/B2 showing helix crossing. a) NMR derived structure b) final frame of Erb-md. Helices run from right to left (N to C-term), and in b) ErbB2 is going into the page. Residue color Green are numbered residues in $^{12}\text{XXX}^{16}\text{SXXX}^{20}\text{G}$, cyan in $^{13}\text{SXXX}^{17}\text{A}$, orange in $^{12}\text{SXXX}^{16}\text{GXXX}^{20}\text{A}$ (Ser12 is only shown in b), red, residues that block rotation to smaller helix-crossing angles (Val19/Leu23 on ErbB2, Leu23 on ErbB1; Ile14 on ErbB2, Ile13 on ErbB1).

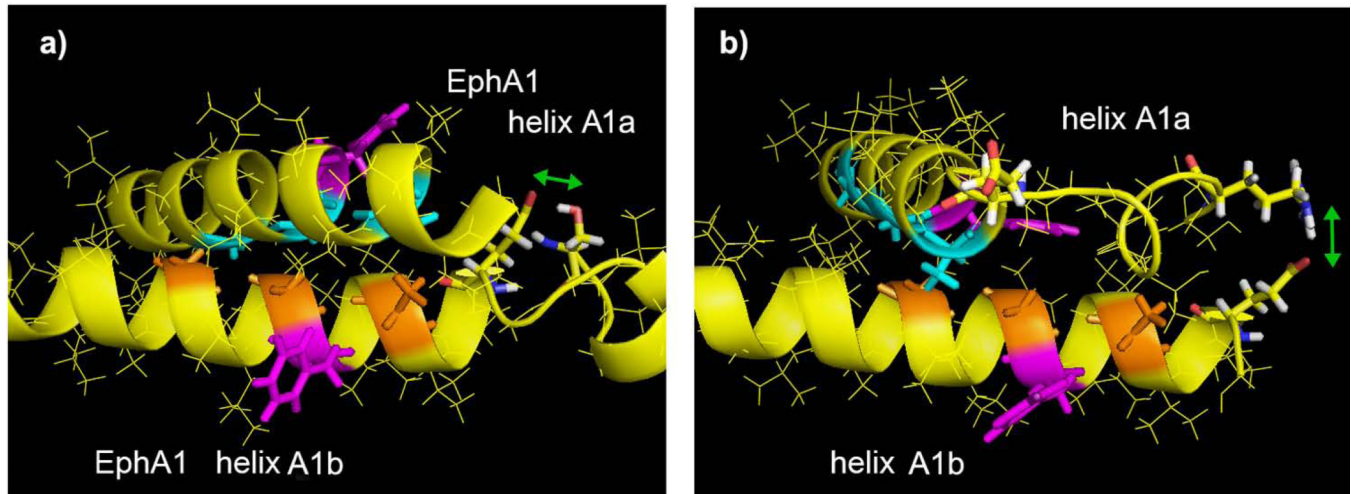


Figure 6.

Region of EphA1 homodimer showing helix crossing. a) NMR derived structure b) final frame of Eph-md. Helices run from right to left (N to C-term), and in b) helix A1a is going into the page. Residue color cyan and orange are numbered residues in $^{15}\text{AXXX}^{19}\text{GXXX}^{23}\text{G}$, magenta – the position of the sidechain of Phe18 is shown to indicate helix orientation. Glu12 is shown at the end of helix A1b in both panels. Glu12 – Ser5 (both on helix A1b) and Glu12 (helix A1b) – Arg6 (helix A1a) sidechain interactions are shown with green arrow.